GOCE DELCEV UNIVERSITY - STIP
FACULTY OF COMPUTER SCIENCE

The journal is indexed in
EBSCO

ISSN 2545-4803 on line
DOI: 10.46763/BJAMI

BALKAN JOURNAL OF APPLIED MATHEMATICS AND INFORMATICS (BJAMI)

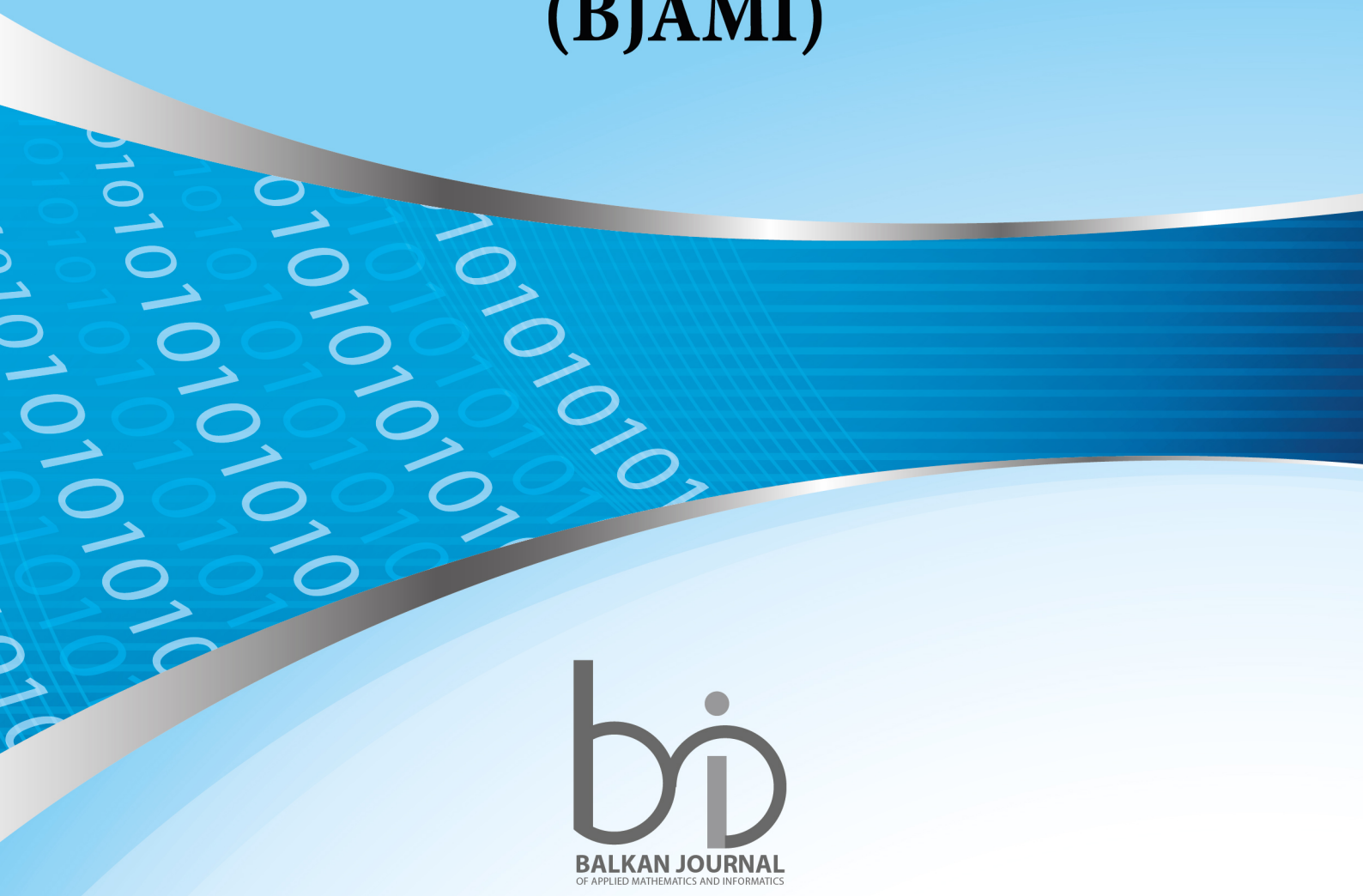

BALKAN JOURNAL
OF APPLIED MATHEMATICS AND INFORMATICS

YEAR 2022

VOLUME V, Number 1

GOCE DELCEV UNIVERSITY - STIP
FACULTY OF COMPUTER SCIENCE

ISSN 2545-4803 on line

BALKAN JOURNAL OF APPLIED MATHEMATICS AND INFORMATICS

(BJAMI)

YEAR 2022 VOLUME V, Number 1

AIMS AND SCOPE:
BJAMI publishes original research articles in the areas of applied mathematics and informatics.

Topics:
1. Computer science;
2. Computer and software engineering;
3. Information technology;
4. Computer security;
5. Electrical engineering;
6. Telecommunication;
7. Mathematics and its applications;
8. Articles of interdisciplinary of computer and information sciences with education, economics, environmental, health, and engineering.

Address of the editorial office
Goce Delcev University – Stip
Faculty of philology
Krste Misirkov 10-A
PO box 201, 2000 Štip,
Republic of North Macedonia

BALKAN JOURNAL
OF APPLIED MATHEMATICS AND INFORMATICS (BJAMI), Vol 3

ISSN 2545-4803 on line
Vol. 5, No. 1, Year 2022

EDITORIAL BOARD

CONTENT

Balkan Journal of Applied Mathematics and Informatics
Volume V Number 1 Year 2022
Online ISSN 2545-4803
UDC: 624.131.522.041.6:517.958

DEPENDENCE OF INPUT ENERGY FROM THE RIGIDITY OF THE FOUNDATION

ALEKSANDRA RISTESKA-KAMCHESKI AND VLADO GICEV AND MIRJANA KOCALEVA

Abstract. In this paper we analyzed a two-dimensional model of the ground-foundation system (construction) and studied how the physical-mechanical characteristics (density and propagation velocity) of the constituent elements of the ground-foundation system affect the energy that will enter the building. We also investigated the influence of the angle of the incoming wave on the propagated energy in the building.
Keywords: foundation, wave propagation, nonlinearity

1. Introduction

In the field of physical phenomena where the region of interest is infinite, such as the case of the problem of propagation of seismic and other types of waves, the application of numerical simulation is impossible and unnecessary to perform throughout the region. In this case, artificial boundaries are introduced to truncate the model in finite sizes. Those artificial limits should be such as to allow the wave to travel freely through the boundaries, in and out of the numerical model. With a truncated model of this kind there is a wide field of research that involves the response of elements with finite dimensions to a seismic wave. According to the action-reaction law, the response is dependent on the input energy. In general, the input energy through a given cross-section depends on the velocity of the particles at equation. Because our point of interest is the response of interactive soil-structure system which interacts through the foundation, our goal was to determine how different factors affect the velocity of the particles at the foundation-object contact, and thus at the seismic energy entering the building. The amplitude of the velocity depends on many aspects, such as mechanical characteristics of the soil and foundation, introduction of the nonlinearity in the computation, the incident angle of the incoming wave θ etc.

The most popular numerical methods for solving wave equation described with partial differential equations are the finite element method and the finite difference method. Typically, the finite element method uses implicit schemes in which unknown quantities at all spatial points are determined simultaneously for each time step by solving a system of linear algebraic equations. Otherwise, more finite difference calculation schemes are explicit, where the solution is determined by the solution of the previous time step and the equations are independent. The final elements as a numerical tool are more convenient than the final differences for modeling complex and irregular models. However, for large-scale problems arising in seismology, for example, explicit schemes are recommended because they are cheaper (require less computer resources) and easier to implement in numerical algorithms. In the last few decades, with the rapid development of computing machines, researchers have been studying the wave phenomena through computer simulations of mathematical models. With these simulations we can predict how the object will respond to seismic excitations. This means determining which locations of the building will have a concentration of stresses and large permanent deformations that can

lead to breakage of the building. In addition to the vulnerability of structures, computer simulations of mathematical models help us to study soil damage.

2. Numerical model

We analyzed a two-dimensional model of a ground-foundation-structure system (construction). The interest of this research was how the physical-mechanical characteristics (density and velocity of propagation) of the constituent elements of the ground-foundation-structure system affect the energy that will enter the building. Because of that, we neglected the geometric details of the building and the foundation and approximated them with rectangles. The building, the foundation, and the soil (ground) have different physical properties. We assumed that the building and the foundation were linear, and that the soil could suffer nonlinear deformation. The nonlinearity of the soil affects the response of the building to excitation at the base. The excitation is from a half-sinusoidal pulse (Fig. 1), and the angle that occupies the direction of propagation of the wave with the vertical is denoted by θ. It is assumed that all the contacts (interfaces) between the building and the foundation, and the foundation and the soil, remain continuous. The height of the building is H_b, and the width W_b=2a. The propagation velocity of the wave in the building is β_b, and the density of the material from which the building is made is ρ_b. The foundation has a depth h_f, a density ρ_f and a velocity of propagation of the wave through it β_f. The soil has a density ρ_s and a velocity of wave propagation through it β_s. In our model we took a section of soil with a length L_m=10a and a width H_m=5a. The depth of the foundation is half the width of the building, h_f=a.

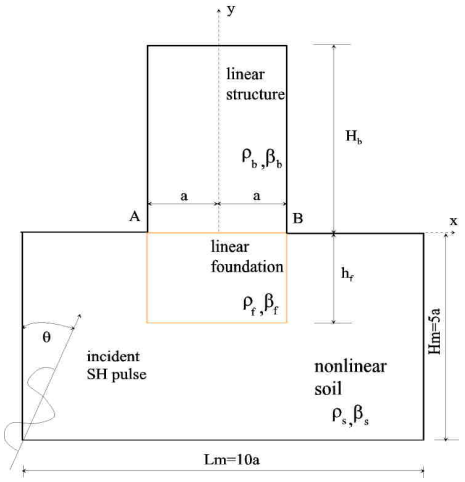

Figure 1. *System with linear structure and foundation and nonlinear soil (Gicev et al, 2015)*

The incoming wave is an SH plane wave in the form of a semisinusoidal pulse and with it we modeled strong impulse movements in the soil. We used the dimensionless frequency $\eta = 2a/\lambda = a/\left(\beta_s \cdot t_{d0}\right)$ as a measure of the pulse duration, where a is half the width of the base, and $\lambda = \mathrm{T} \cdot \beta_s = 2 \cdot \beta_s \cdot t_{d0}$ is the length of the input wave. $T = 2 \cdot t_{d0}$ is the pulse period, β_s is the propagation velocity of the wave in the soil and t_{d_0} is the pulse duration.

For completeness, we will briefly summarize the model of finite differences and its characteristics. To set the spatial network in the finite difference model, we analyze the pulse in a spatial domain (S) and the displacement at the points obtained because of the pulse is:

$$w(s) = A\sin[(\pi \cdot s / (\beta_s \cdot t_{d0}))] \qquad (1)$$

where A is the pulse amplitude and s is the distance from the point under consideration to the front of the wave at the initial time and in the direction of its propagation. Using the fast Fourier transform, the semisinusoid pulse (1) is transformed into a domain of a wave number or spatial frequency (k), as follows:

$$w(k) = F\left[w(s)\right] \qquad (2)$$

The maximum response occurs at $k = 0$ (rigid body motion). As it increases k, the answer $w(k)$ decreases (weakens) and approaches zero, approaching k to infinity. Since $\omega = \beta \cdot k$ and $\lambda = 2\pi / k$ with increasing k the angular frequency ω increases and the wavelength λ decreases. For proper discretization of the grid, i.e., correct interval selection, the highest mode must be selected (max k, i.e., min λ) so that our grid can reproduce well. In this analysis we chose the maximum wave number, $k = k_{\max}$, for which the answer $w(k)$ is at least 0.03 of the maximum, $w(0)$ (Gicev, 2008). Then, for this value of $k_{\max}$, the corresponding frequencies and wavelengths are:

$$\omega_{\max} = k_{\max}\beta \text{ and } \lambda_{\min} = 2\pi / k_{\max} = 2\pi\beta / \omega_{\max} \qquad (3)$$

where $\beta = \beta_S$ is the propagation velocity of the wave in the soil.

The accuracy of the finite difference network depends on the ratio of the numerical and physical propagation velocities, c / β which ideally should be 1. The parameters that affect this accuracy are:

1) The density of the network $m = \lambda / \Delta x$ (m is the number of wavelength points λ, and Δx is the distance between points in the grid);
2) Courant number $\chi = \beta_s \Delta t / \Delta x$ (Δt is a time step);
3) The angle of the input wave θ.

It has been shown that the error increases when m and χ decrease and θ is close to 0 or $\pi / 2$ (Alford et al., 1974; Fah, 1995; Dablain, 1986). For a second order approximation, the above authors state $m = 4$.

To model the soil numerically, we selected a rectangular section with the dimensions $L_m = 10a$ and $H_m = L_m/2 = 5a$ (Figure 1). For practical reasons, the maximum number of spatial intervals in the network in the horizontal direction (x-axis) is 200, and in the vertical (y-axis) 400 (125 in the soil plot and 275 in the building). The minimum spatial intervals in the model are $\Delta x_{\min} = L_m / 200 = 76.4 / 200 = 0.382\ m$. For a grid with a smaller spatial interval Δx, the computation time increases rapidly. Thus, for $\eta = 2$, according to the above-mentioned criterion for discretization, the highest mode that we want to be well reproduced with our spatial grid has a wave number $k = k_{\max}$ for which $w(k) \approx 0.03 \cdot w_{max} = 0.03 \cdot w(0)$ has a frequency $\omega_{\max} = 980\ rad / s$.

3. Energy distribution in the system

The flow of energy through a given area can be defined in relation to the passage of the wave through the surface A_{sn}:

$$E_{in}^{a} = \rho_s \cdot \beta_s \cdot A_{sn} \cdot \int_0^{t_{d0}} v^2 \cdot dt \qquad (4)$$

Where ρ_s is the density of the soil, β_s is the velocity of propagation of the wave through the soil, v is the velocity of movement of soil particles, and A_{sn} is the area normal to the direction of wave propagation. From the geometry of our calculation model (Figure 1), the area normal to the passing wave is:

$$A_{sn} = 2 \cdot H_m \cdot \sin\gamma + L_m \cdot \cos\gamma = L_m \cdot (\sin\gamma + \cos\gamma) \qquad (5)$$

where H_m is the height and L_m width of the soil section in our model (Figure 1), respectively. By inserting and integrating equations (3) in (2), we get the analytical solution for the wave energy input in the model, as follows:

$$E_{in}^{a} = \rho_s \cdot \beta_s \cdot L_m \cdot (\sin\gamma + \cos\gamma) \cdot (\pi A / t_{d0})^2 \cdot t_{d0} / 2 \qquad (6)$$

As can be seen from equation (6), for the defined length of the soil section L_m and the defined input angle γ, the input energy is reciprocal of the pulse duration, which means that it is a linear function of the dimensionless frequency η. Due to the law of conservation of energy, the input energy is balanced by the following:

- Cumulative energy E_{out} goes out of the model, and is calculated by equation (4),
- Cumulative (hysterical) energy, i.e., the energy consumed for the creation and development of permanent deformations in the soil, is calculated by:

$$E_{hys} = \sum_{t=0}^{T_{end}} \Delta t \cdot \sum_{i=1}^{N} \left(\sigma_{xi} (\Delta\varepsilon_{xpi} + 0.5 \cdot \Delta\varepsilon_{xei}) + \sigma_{yi} (\Delta\varepsilon_{ypi} + 0.5 \cdot \Delta\varepsilon_{yei}) \right), \qquad (7)$$

where T_{end} is the time at the end of the analysis, N is the total number of points, σ_{xi}, σ_{yi} are the stresses at points in x and y axis, respectively, $\Delta\varepsilon_{xpi} = \varepsilon_{xpi}^{t+\Delta t} - \varepsilon_{xpi}^{t}$ is the increase of the elastic deformation in the direction x at point i, and $\Delta\varepsilon_{yei} = \varepsilon_{yei}^{t+\Delta t} - \varepsilon_{yei}^{t}$ is the increase of the elastic deformation in the direction y at the point i.

- The instantaneous energy in a building, which consists of kinetic and potential energy, can be calculated from:

$$E_b = E_k + E_p = 0.5 \cdot \Delta x \cdot \Delta y_b \cdot \sum_{i=1}^{N} \left(\rho \cdot v_i^2 + \mu \cdot (\varepsilon_x^2 + \varepsilon_y^2) \right) \qquad (8)$$

where Δx and Δy_b are the horizontal and vertical distances of the grid in the building, ρ and μ are the density and shear modulus of the building, respectively, v_i is the velocity of the particles, while ε_x and ε_y are the deformations at point i of the building.

To study only the effect of scattering on the foundation, it is assumed that the building is high enough so that the reflected wave from the top of the building cannot reach the building-foundation contact by the end of the analysis. The analysis is stopped when the wave is completely out of the ground.

4. Numerical example

We took the Holiday Inn Hotel in Van Nuys, California as a prototype for our two-dimensional numerical model (Figure 2). The hotel is located in the middle of the San Fernando Valley in the metropolitan area of Los Angeles, California, and was fully instrumented. During the Northridge earthquake in California in 1994, the hotel was severely damaged (Figure 3) and its response during this earthquake has been analyzed and described in many articles and reports (Li and Jirsa, 1998; Browning et al., 2000); Trifunac and Ivanovic, 2003; Gicev and Trifunac 2006; Gicev and Trifunac 2011. For our two-dimensional SH model, we took the physical-mechanical characteristics of the soil on which the hotel is built, as well as the equivalent physical-mechanical characteristics of the hotel in the east- west, obtained by impulse response analysis of a one-dimensional model.

Figure 2. *View of the hotel "Holiday Inn" Nuys from North-East*

Figure 3. *Post-earthquake view of in Van damaged columns*

We assumed that all contacts in our model, three foundation-soil contacts and one foundation-building contact (Figure 1), remain continuous, i.e., no separation or sliding is allowed. The building and the foundation remain linear throughout the analysis. Figure 1 shows the dimensions of the model and the physical-mechanical characteristics of the elements that make up the model in general numbers. For our example, the propagation velocity of the SH wave in a building is $\beta_b = 100\, m/s$, $\beta_s = 250\, m/s$ in the ground. The width of the foundation is the same as the width of the building $W_b = 2a = 19.1m$, and its depth is half of its width, $h_f = a = 9.55\, m$. The density of the material from which the building is constructed is $\rho_b = 270\, kg/m^3$ for all examples in this study. We took the density of the foundation and the soil the same $\rho_f = \rho_s = 2000\, kg/m^3$.

We stop the calculation at time *Ts*, when the complete filtered pulse passes the right corner of the foundation-structure contact, B (Figure 1).

$$T_s = \frac{H_m}{c_y} + \frac{\frac{L_m}{2} + a}{c_x} + t_d = \frac{H_m}{c_y} + \frac{6a}{c_x} + t_d, \qquad (9)$$

Where $c_y = \frac{\beta_s}{\cos\gamma}$ and $c_x = \frac{\beta_s}{\sin\gamma}$ are the vertical and horizontal phase velocities of the SH wave propagating in the soil, L_m and H_m (Figure 1) are the width and height of the soil section, a is the half-width of the structure and t_d is the duration of the half-sinusoidal pulse. After this time, we have no energy input in the construction. Since we only researched the energy that enters the construction, we varied the height of the building, H_b. We calculated the height of the building from the condition for the time after the wave front (pulse) that reached point A (Figure 1), reached the top of the structure, bounced and continued to travel backwards, did not reach the foundation-building contact until the moment when the complete pulse had passed point B when we interrupted the numerical simulation. The shortest time to reach the wavefront from the lower left corner of the model to the left corner of the foundation contact, then bounce off the top of the structure and reach the foundation contact again is:

$$T_r = \frac{H_m}{c_y} + \frac{\frac{L_m}{2} - a}{c_x} + \frac{2H_b}{\beta_b} = \frac{H_m}{c_y} + \frac{4a}{c_x} + \frac{2H_b}{\beta_b} \qquad (10)$$

Then the required condition for calculating the height of the building is $T_r \geq T_s$, or

$$\frac{H_m}{c_y} + \frac{4a}{c_x} + \frac{2H_b}{\beta_b} \geq \frac{H_m}{c_y} + \frac{6a}{c_x} + t_d \qquad (11)$$

From (11) and keeping in mind that $c_x = \frac{\beta_s}{\sin\gamma}$, we calculate the required height of the structure (object) $H_b \geq \frac{a \cdot \sin\gamma \cdot \beta_b}{\beta_s} + \frac{t_d \cdot \beta_b}{2}$. From the point of view of design of seismically resistant structures, it is important to know the excitation at the base of the structure. Because the input energy through a given cross-section depends on the velocity of the particles at equation (11), we investigated how different factors affect the velocity of the particles at the foundation-object contact, and thus at the seismic energy entering the building. The factor that we researched was the level of nonlinearity of the ground C, at different input angles θ. For this purpose, we have defined the mean velocity of the particles of the contact object-foundation:

$$v_{av} = \frac{\sum_{i=1}^{N_c} v_i}{N_c}, \qquad (12)$$

where N_c is the number of points of the contact foundation-object, and v_i is the velocity at point *i* of the contact in time step *k*. In this way, for each time step of our numerical simulation, we calculated the mean pulse excitation velocity with a dimensionless frequency η. For the largest absolute value of the mean velocity and the corresponding η, we obtain a point on the curve $v_{av,\max}(\eta,t)$. We conducted the research in the domain of the dimensionless frequency of excitation $0.06 \le \eta \le 3$ with a step $\Delta\eta = 0.02$. In this way we have $N_p = \frac{3-0.06}{0.02} + 1 = 148$ points on our curves $v_{av}(\eta)$.

5. Results and discussion

Fig. 4 shows the above-mentioned curves for the vertical input of the excitation, θ = 0. From the picture it can be seen that the models without foundation, i.e., models where the stiffness of the foundation is equal to the stiffness of the ground, $\beta_f=\beta_s=250$ m/s (point lines), have the highest relative average velocity. For such rigidity of the foundation, for the model with the soil with the lowest level of nonlinearity, C = 1.5 (blue line), there are the largest ordinates. The model without foundation, with the soil with nonlinearity level, C = 1.1 (green dot line), for the longest pulses, η = 0.06 to η = 0.48, has the same ordinances as the model with the soil with nonlinearity level C = 1.5 which had a local minimum in this η. The model with C = 1.1 has a minimum $v_{av,r}(\eta)=0.859$ for η = 0.58, and further by increasing η, it goes parallel to the curve with the level of nonlinearity C = 1.5. The maximum $v_{av,r}(\eta)=0.898$ occurs at η = 1.2, and for η=3, $v_{av,r}(\eta)$= 0.868. The model with the largest nonlinearity on the ground, C = 0.8 (red dot line), follows the trend of the previous two curves, but $v_{av,r}(\eta)$ is not starting from 1 for the smallest considered dimensionless frequency, but from $v_{av,r}(\eta)$= 0.8. This is because in the previous two curves, for the smallest dimensionless frequencies, the ground is linear and there is no permanent deformation in it, which is not the case with the model with large nonlinearity, C = 0.8, when permanent deformations occur at the smallest η.

Curves $v_{av,r}(\eta)$ for mathematical models with foundations stronger than the ground, β_f = 500 m / s; 1000 m / s (dashed and solid lines respectively) behave similarly to the model curves without foundation $\beta_f = \beta_s$ = 250 m / s, with the difference that their ordinates are smaller. This is due to the fact that the foundation dissipates energy when the pulse beats in it. Because the model without foundation, $\beta_f = \beta_s = 250$ m / s does not scatter energy, all the energy from the pulse comes to the contact "foundation" -object and therefore the ordinates in these models are larger than in the models with a foundation stiffer than the ground. Again, models with low nonlinearity on the ground have larger ordinates than models with higher nonlinearity.

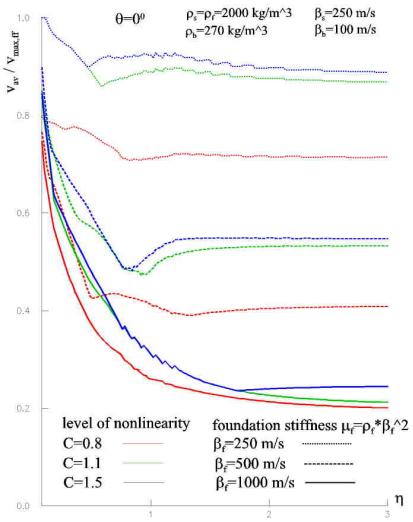

Figure 4. *Peak average velocity v_{av} at structure-foundation interface normalized by peak free-field velocity $v_{max,ff}$ vs. η for three foundation stiffness and three levels of nonlinearity of soil. $\theta = 0^0$*

The model with the hardest foundation $\beta_f = 1000$ m / s and with the highest level of nonlinearity in the ground C = 0.8 (red solid line) has the smallest ordinates of all η, which leads to the conclusion that the models with a rigid foundation and high nonlinearity in the soil, i. e., small ε_m, i.e., small C in equation (6), prevent (do not allow) much of the energy to reach the object (to the foundation-object contact). This insight allows us to understand why many of the buildings on weak soil (with a high level of nonlinearity), and close to the epicenter of Northridge, 1994 earthquake remained completely undamaged. On the other hand, it is clear that rigid foundations lead to strong scattering of the waves that hit them, so that a large part is scattered, and a small part of the seismic energy enters the foundation, and from there to the contact foundation. As the input angle θ increases, so for high frequencies (to the right of Figures 6.7 to 6.9, the curves $v_{av,r}(\eta)$ approach. Figure 5 shows the corresponding curves for the input angle θ = 30^0. It can be seen that for small dimensionless frequencies (e.g. for $\eta \leq 1$ ordinates the curves $v_{av,r}(\eta)$ for the models with the foundation $\beta_f = 250 m/s$ and $\beta_f = 500 m/s$ (dotted and dashed lines) get closer to each other while the curves for the models with the foundation $\beta_f = 1000\, m/s$ they remain further apart.

Figure 6 shows the curves $v_{av,r}(\eta)$ for the entry angle θ = 60^0. From the figure it can be seen that for small η, the model without foundation $\beta_f = \beta_s$ =250 m / s with the lowest level of nonlinearity on the ground C = 1.5 has the highest value for the average velocity. For $\eta = 0$, i.e., for the longest pulses, $v_{av,r}(\eta)$ has the ordinate close to 0.86 and as the dimensionless frequency increases, $v_{av,r}(\eta)$ decreases sharply. At $\eta = 0.5$ the relative

velocity of the model with foundation $\beta_f = 500$ m / s (dashed line) and with the lowest level of nonlinearity on the ground C = 1.5, it becomes greater than the same for $\beta_f = \beta_s$ =250 m / s and C = 1.5. For $\eta > 0.5$ the relative velocities for this model are the highest and for $\eta = 3$ reach the lowest value in the considered interval, about 0.25. The model without foundation, with the level of nonlinearity on the ground C = 1.1 for $\eta = 0$ has a maximum ordinate for the relative velocity 0.8. The curve of this model runs parallel to the curve with the level of nonlinearity C = 1.5 and the minimum occurs for $\eta = 3$, $v_{av,r}(\eta) = 0{,}24$ (dashed line, $\beta_f = 500$ m / s). The model with the largest nonlinearity on the ground (red dot line) behaves similarly to the previous curve, with the minimum value for the average velocity reaching the same for $\eta = 3$, $v_{av,r}(\eta) = 0{,}2$.

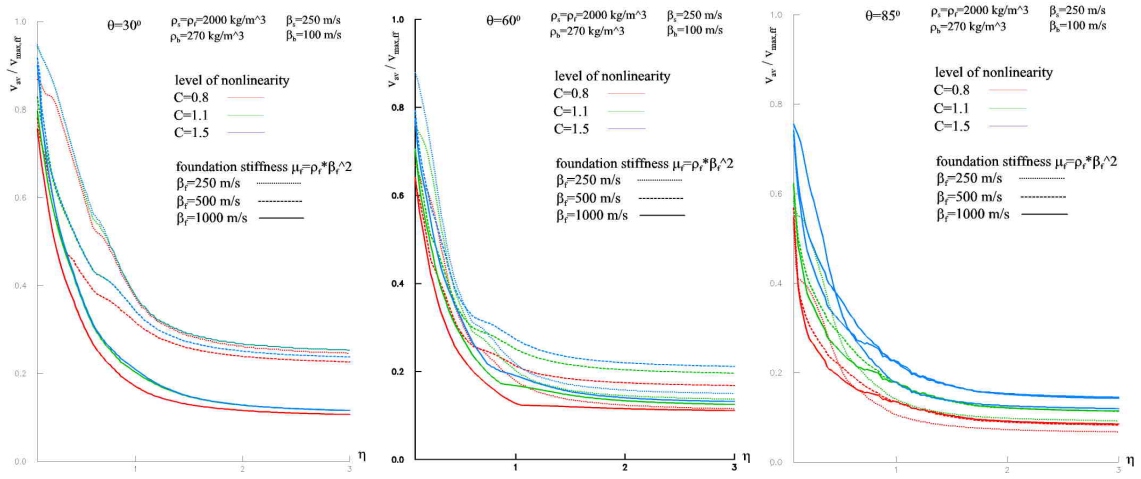

Same as Fig.4 but for **Figure 5.** $\theta = 30^0$ **Figure 6.** $\theta = 60^0$ **Figure 7.** $\theta = 85^0$

The curves $v_{av,r}(\eta)$ for models with foundations stronger than the ground, $\beta_f = 500$ m / s and $\beta_f = 1000$ m / s (solid lines respectively) behave like the curves for the model without foundations, with the difference that their ordinates are smaller (for C = 1.5 the ordinance is 0 , 8, for C = 1.1 the ordinate is 0.7, and for C = 0.8 the relative velocity has the lowest value around 0.65). The reason is that the foundation dissipates energy when the pulse beats in it, while in the model without the foundation all the energy from the pulse is missed and that is why the ordinances of this model have higher values for velocity. It is observed that the increase of the input angle leads to the approximation of the curves $v_{av,r}(\eta)$. The curves with foundation $\beta_f = \beta_s = 250$ m / s and $\beta_f = 1000$ m / s (point and solid lines) are closer to each other for $1.5 \le \eta \le 3$, while for $\beta_f = 500$ m / s the curves remain further apart in the same interval.

Figure 7 shows the curves of the previous mathematical models, but at the input angle of the pulse $\theta = 85^0$. It is obvious that the maximum value for the relative velocity $v_{av,r}(\eta)$

is lower than that at the input angle θ = 60^0, $v_{av,r}(\eta) = 0{,}75$. This value reaches the curve of the model without foundation ($\beta_f = \beta_s$ = 250 m / s) for the lowest nonlinearity of the ground C = 1.5 (blue dot line). The highest order of the curve of the model is closer with a firmer foundation than the ground (β_f = 500 m / s) and the same level of nonlinearity (blue dashed line). The average velocity at both curves decreases with increasing dimensionless frequency, and in the interval $1 \le \eta \le 3$ they almost coincide, reaching the minimum value $v_{av,r}(\eta) = 1{,}97$ for $\eta = 3$. Curves with the level of nonlinearity C = 1.1 behave similarly for all three models of rigidity of the foundation, with a small difference in the maximum and minimum of the relative velocity. The largest order reaches the curve of the model without foundation (green dotted line), about 0.73, and the lowest value around 0.1. Fig. 7 also shows that, as the input angle of the pulse θ increases, with increasing frequency, the curves $v_{av,r}(\eta)$ decrease and approach each other (some of them even coincide). This shows that at higher η the rigidity of the foundation and the degree of nonlinearity of the ground are almost irrelevant to the values of the relative velocity of the foundation-object contact $v_{av,r}(\eta)$. It is also obvious that these velocities for larger η become almost constant, i.e., they no longer depend on the frequency.

6. Conclusion

We come to the conclusion that the models with high nonlinearity on the ground have the smallest ordinates for $v_{av,r}(\eta)$, i.e., as the nonlinearity of the ground increases, so most of the input energy is scattered from the foundation, and a smaller part enters the building. The model with the hardest foundation and the highest level of nonlinearity in the ground prevents (does not allow) much of the energy to reach the object (to the foundation-object contact). This knowledge allows us to understand why many of the objects on weak soil (with a high level of nonlinearity). On the other hand, it is clear that rigid foundations lead to strong scattering of the waves that hit them, so that a large part is scattered, and a small part of the seismic energy enters the foundation, and from there to the contact foundation. We concluded that, as the foundation becomes stronger, much of the input energy is scattered from the foundation, and a smaller part enters the building.

References

[1] *Li, Y.R., and Jirsa, J.O.* (1998). Nonlinear analyses of an instrumented structure damaged in the 1994 Northridge earthquake, *Earthquake Spectra*, *14*(2), 265–283.

[2] *Browning, J.A., Li, R.Y., Lynn, A., and Moehle, J.P.* (2000). Performance assessment for a reinforced concrete frame building. *Earthquake Spectra*, *16*(3), 541–555.

[3] *Trifunac, M.D., and Ivanovic, S.S.* (2003). Analysis of Drifts in a Seven-Story Reinforced Concrete Structure, *Dept. of Civil Eng. Report No. CE 03-01*, Univ. of Southern California, Los Angeles, California.

[4] *V. Gicev and M.D. Trifunac* (2006). Non-linear earthquake waves in seven-story reinforced concrete hotel, Report CE 06-03

[5] *Gicev, V. and Trifunac, M.D.* Asymmetry of nonlinear soil strains during soil-structure interaction excited by SH pulse, *Izgradnja*, vol. 66, br. 5-6, 2012, 129-148
[6] *Vlado Gicev, Mihailo D. Trifunac, Nebojsa O.* - Translation, torsion, and wave excitation of a building during soil-structure interaction excited by an earthquake SH pulse, Soil Dynamics and Earthquake Engineering, vol. 77, 2015, 391-401.
[7] *Vlado Gicev, Mihailo D. Trifunac, Nebojsa O.* - Two-dimensional translation, rocking, and waves in a building during soil-structure interaction excited by a plane earthquake P-wave pulse, Soil Dynamics and Earthquake Engineering, vol.90, 2016, 454-466.
[8] *Vlado Gicev, Mihailo D. Trifunac, Nebojsa O.* - Two-dimensional translation, rocking, and waves in a building during soil-structure interaction excited by a plane earthquake SH-wave pulse, Soil Dynamics and Earthquake Engineering, vol. 88, 2016, 76-91.
[9] Analiza parametara za procenu seizmickog odgovora visespratnih armiranobetonskih okvira, Aleksandra Radujkovic, Doktorska disertacija, Novi Sad, 2015.
[10] Privremeni tehnički propisi za opterećenja zgrada (1948).
[11] Abramowitz M. and Stegun I.A. (1965), Handbook of mathematical functions, Dover, New York.
[12] Achenbach J. D. *1973), Wave propagation in elastic solids, Noth - Holland, Amsterdam.
[13] Alford R.M, Kelly K.R. and Boore D.M. (1974), Accuracy of finite-difference modeling of acousticwave ecuation, Geophysics v.39, 834-842.
[14] Alterman Z.S and Karal F.C. Jr (1968), Propagation of elastic waves in layered media by finite-difference methods, BSSA vol. 58, 367-398.
[15] Boore D. M. (1970), Finite-difference solutions to the equations of elastic wave propagation, with applications to Love waves over dipping interfaces; PhD thesis M.I.T.
[16] Byrne P. M. (1980), Seismic response of buildings on soft foundation soils, 7th World conference on earthquake engineering, Vol. 6, 29-96.
[17] Chew W. C. and Wagner R. L. (1992), A modified form of Liao's absorbing boudnary condition, IEEE AP-S/URSI Int. Symp. Dig., Chicago IL, 536-539.
[18] Clayton R. and Engquist B. (1977), Absorbing boundary conditions for acoustic and elastic wave equations, BSSA vol. 67, 1529-1540.
[19] Clearbout J. F. and Johnson A. (1971), Extrapolation of time dependent wave forms along their path of propagation, Geophysics J. of Royal Astron. Soc, 285-293.
[20] Ditkowski A. and Gottlieb D., (2002), On the Engquist Majda absorbing boundary conditions for hyperbolic system, Division of applied mathematics, 1-23.
[21] Engquist B., Majda A. (1977), Absorbing boundary conditions for the numerical simulation of waves, Math. Comp. 31, 629-651; Univ. of Southern California, Los Angeles, CA.
[22] Gicev V. and Trifunac M. (2007), Energy and power of nonlinear waves in seven story reinforced concrete building, Soil Journal of Indian Society of Earthquake Technology, vol.44 (1.1), 305-323.
[23] Gicev V. and Trifunac M. (2011), A note on predetermined earthquake damage scenarios for structural health monitoring, Structural control, and health monitoring, 19, 746-757.
[24] Grote M.J. and Keller J.B. (1996), Nonreflecting boundary conditions for time-dependent scattering, Journal of Computational Physics 127, 52-65.
[25] Grote M.J. and Kirsch C (2004), Dirichlet-to-Neumann boundary conditions for multiple scattering problems, Journal of Comput. Phys 201 (6.2), 630-650.
[26] Grote M.J. and Kirsch C (2007), Nonreflecting boundary condition for time -dependent mulitple scattering, Journal of Comput. Phys 221 (1.1), 41-62.
[27] Kallivokas L.F and Lee S. (2004), Local absorbing boundaries of elliptical shape for scalar waves, Comp. Methods in Appl. Mech. and Eng. 193, 4979-5015.
[28] Kausel E. (1974), Forced vibration for circular foundations on layared media. M. L. T. Research report, Soils publications No. 336.
[29] Kausel E. and Tassoulas J.L (1981), Transmittign boundaries: A close-form comparison, BSSA Am., 71(1.1), 143 – 159.
[30] Liao Z.P., Wong H.L. (1984), A transmiting boundary for the numerical solution of elastic wave propagation, Soil Dynamics and Earhtquake Eng. 3, 174-183.
[31] Lysmer J. and G. Waas (1972), Shear waves in plane infinite structures, J.Eng. Mech. Div., ASCE 98, 85-105.

[32] Lysmer J. and Kuhlemeyer R. L. (1969), Finite-dynamic model for infinite media, J. Eng. Mech. Div. 95(4), 859-877.
[33] Priestly M. J. N., Evison R. J.and Carr A. J., Seismic response of structures free to rock on their foundations, Bulletin of the New ZeNational Society of Earthquake Engineering, Vol.11 No. 3, 141-150.
[34] Smith W.D. (1974), A non-reflecting plane boundary for wave propagation problems, Journal of Computational Physics 15, 492-503.
[35] Simmerfield A. (1912), Die Greensche Funktion der Schwingungsgleichung, Jber Deutschen Math. Verein 21, 309-353.
[36] Stacey R. (1991), An explicit unstable mode in the Clayton and Engquist transparent boundary prescription, BSSA vol.81 no.2, 694-698.
[37] Stacey R. (1988), Improved transparent boundary formulations for the elasticwave equation, BSSA vol.78 no.6, 2089-2097.
[38] Todorovska M, Trifunac M. (2006), Impulse response analysis of the Van Nuys 7-story hotel during 11 earthquakes (1971-1994): one-dimensional wave propagation and inferences on global and local reduction of stiffness due to earthquake damage, Report CE06-01, Dept. of Civil Eng., University of Southern California, Los Angeles, California.
[39] Tsynkov S.V. (1998), Numerical solution of problems on unbounded domains. A review, Applied Numerical Mathematics 27, 465 – 532.
[40] Waas G. (1972), Linear two - dimensional analysis of soil dynamic problems in semi - infinite layered media, Phd dissertation.
[41] Wagner R.L and Chew W.C. (1995), An analysis of Liao's Absorbing boundary condition; journal of Electromagnetic Waves and Applications vol.9 no. 7- 8, 993-1009.
[42] Gicev, V. and Trifunac, M.D. Permanent Deformations and Strains in a Shear Building Excited by a Strong Motion Pulse. Soil Dynamics and Earthquake Engineering, vol. 27, issue 8, August 2007, 774-792.
[43] Gicev, V. and Trifunac, M.D. Rotations in a shear beam model of a seven-story building caused by nonlinear waves during earthquake excitation, Structural Control and Health Monitoring, vol. 16 (4),460-482, 2009, Published Online: Jul 8 2008 DOI:10.1002/stc264.
[44] Gicev, V. and Trifunac, M.D. Transient and permanent rotations in a shear layer excited by strong earthquake pulses, Bulletin of the Seismological Society of America, vol. 99 (2B), 2009, 1391-1403.

Aleksandra Risteska-Kamcheski
University of Goce Delcev, Stip,
Republic of North Macedonia
Faculty of Computer Science
E-mail address: aleksandra.risteska@ugd.edu.mk

Vlado Gicev
University of Goce Delcev, Stip,
Republic of North Macedonia
Faculty of Computer Science
E-mail address: vlado.gicev@ugd.edu.mk

Mirjana Kocaleva
University of Goce Delcev, Stip,
Republic of North Macedonia
Faculty of Computer Science
E-mail address: mirjana.kocaleva@ugd.edu.mk